Applied Surface Science 257 (2011) 10789–10794

Contents lists available at ScienceDirect

Applied Surface Science

journal homepage: www.elsevier.com/locate/apsusc

Photoluminescence and photoelectrochemical properties of nanocrystalline ZnO thin films synthesized by spray pyrolysis technique

N.L. Tarwal, V.V. Shinde, A.S. Kamble, P.R. Jadhav, D.S. Patil, V.B. Patil, P.S. Patil*

Thin Film Materials Laboratory, Department of Physics, Shivaji University, Vidyanagar, Kolhapur 416 004, Maharashtra, India

ARTICLE INFO

Article history:
Received 30 January 2011
Received in revised form 6 July 2011
Accepted 24 July 2011
Available online 29 July 2011

Keywords:
Zinc oxide thin films
X-ray diffraction
Optical properties
Photoluminescence

ABSTRACT

A simple and inexpensive spray pyrolysis technique (SPT) was employed for the synthesis of nanocrystalline zinc oxide (ZnO) thin films onto soda lime glass and tin doped indium oxide (ITO) coated glass substrates at different substrate temperatures ranging from 300 °C to 500 °C. The synthesized films were polycrystalline, with a (0 0 2) preferential growth along *c*-axis. SEM micrographs revealed the uniform distribution of spherical grains of about 80–90 nm size. The films were transparent with average visible transmittance of 85% having band gap energy 3.25 eV. All the samples exhibit room temperature photoluminescence (PL). A strong ultraviolet (UV) emission at 398 nm with weak green emission centered at 520 nm confirmed the less defect density in the samples. Moreover, the samples are photoelectrochemically active and exhibit the highest photocurrent of 60 μA, a photovoltage of 280 mV and 0.23 fill factor (FF) for the Zn_{450} films in 0.5 M Na_2SO_4 electrolyte, when illuminated under UV light.

1. Introduction

ZnO, a direct and wide band gap (~3.37 eV) semiconductor with wurtzite structure, has attracted considerable attention due to its good optical, electrical, piezoelectrical properties and its potential applications in diverse areas such as optoelectronics, transducers, resonators [1], solar cells [2–4], gas sensors [5], transparent conductors [6], etc.

Several deposition techniques have been employed to deposit ZnO thin films such as solid–vapor process [1], solution approach [2], metal organic chemical vapor deposition [3], thermal evaporation [4], chemical bath deposition [5] and SPT [7–17]. Among these methods, the SPT [7] is a popular technique which is very simple, low cost and easily scalable. The control over ZnO properties and tuning their morphologies can be easily accomplished through judicious optimization of the preparative parameters of the SPT. The properties are mainly dependent on the various parameters like nature of the precursor solution, solution concentration, solution quantity, nozzle geometry, mono-dispersion of sprayed droplets and subsequent aerosols, effective pyrolytic decomposition, highly uniform substrate/deposition temperature, local cooling of substrate during spray, spray rate, nozzle to substrate distance and deposition time. Thus, these preparative parameters in case of SPT need optimization in order to achieve desired properties of the films.

Some recent studies [8–17] showed that the substrate temperature is a crucial parameter that has a strong influence on the properties of SPT derived ZnO thin films. It influences solvent evaporation, solute precipitation, the extent of pyrolytic decomposition, nucleation and growth of the thin films [17].

Nowadays, the transition metal oxides (TiO_2, ZnO, WO_3) based photoelectrochemical (PEC) systems have received extensive attention in solar cell applications [18,19]. However, most of the currently studied metal oxides have band gaps that are too wide to absorb the major part of the solar spectrum efficiently. The improvement in the PEC performance of the ZnO thin films was reported by employing several ideas [20–23].

There are several reports available in the literature, which are related to the texture, growth temperature, concentration of the zinc salts in the solution, etc. but the development of both photoluminescent as well as PEC active material has not been thoroughly studied. In the present work, we report the structural, morphological and optical properties of the ZnO thin films deposited at different substrate temperatures by SPT. The PL spectra of the all samples are presented and discussed. Also, the PEC performance of the samples deposited at different substrate temperatures was studied by using a conventional three electrodes system.

2. Experimental

In our previous study [24], we have studied concentration dependent properties of spray deposited ZnO thin films and optimized the solution concentration (0.4 M). In the present study, ZnO thin films were deposited onto the preheated, ultrasonically

* Corresponding author. Tel.: +91 231 2609230; fax: +91 231 2691533.
E-mail address: psp_phy@unishivaji.ac.in (P.S. Patil).

0169-4332/$ – see front matter © 2011 Elsevier B.V. All rights reserved.
doi:10.1016/j.apsusc.2011.07.099

Table 1
Optimum spray conditions for the deposition of ZnO thin films.

Spray parameters	Optimized value
Zinc acetate solution concentration	0.4 M
Substrate temperature	450 °C
Carrier gas	Compressed air
Solution quantity	40 cm^3
Solution spray rate	5 cm^3 min^{-1}
Angular substrate to nozzle distance	22 cm

cleaned glass substrates and ITO coated glass substrates by SPT from an aqueous zinc acetate precursor solution (0.4 M), at different substrate temperatures. The substrate temperature for the ZnO thin films was varied from 300 °C to 500 °C with the steps of 50 °C and the deposited thin film samples are denoted as Zn_{300}, Zn_{350}, Zn_{400}, Zn_{450}, Zn_{500}, respectively. During the synthesis, various preparative parameters like solution spray rate, nozzle to substrate distance, carrier gas flow rate, etc. were optimized in order to obtain transparent, uniform, adherent and pin hole free deposits, are shown in Table 1.

Compressed air was used to atomize the solution containing the precursor compounds through a spray nozzle over the preheated substrate. In the present work, the aqueous zinc acetate precursor solution was pyrolyzed onto the preheated substrates. The substrate holder is equipped with thermocouples and heating elements are equipped with a temperature controller. The spray nozzle consists of two concentric glass pipes, through the inner pipe flows the solution and between inner and outer the air stream; the spray is produced by the Ventury effect at the end of both pipes. To and fro motion of the nozzle was controlled by stepper motor, which is connected to the electronic kit. Hazardous fumes evolving at the time of deposition were succeeded out using external exhaust system connected to the deposition chamber.

Aqueous solution of zinc acetate, when sprayed over the hot substrates, fine droplets of solution thermally decompose after falling over the hot surface of substrates. This results in the formation of well adherent and uniform ZnO films. These films were further used to investigate the structural, morphological, optical and PEC properties. The film thickness of all the samples was measured by Ambios XP-1 surface profiler. The structural and morphological characterizations were carried out using Philips PW 3710 X-ray diffractometer with CuKα radiation (wavelength 1.5405 Å) and scanning electron microscopy (SEM) JEOL JSM-6360, respectively. The optical characterization was carried out using UV–vis Systronics-119 spectrophotometer over the wavelength range 350–850 nm. The PL studies have been investigated using Perkin Elmer LS-55 having Xenon as an excitation source. PEC study was performed in a conventional three-electrode arrangement with the deposited thin film as a working electrode, a graphite counter electrode and SCE as a reference electrode. A 0.5 M Na_2SO_4 aqueous solution was used as an electrolyte. The PEC characteristics were measured under constant ultraviolet illumination of 5 mW cm^{-2} from an 18 W UV lamp with excitation wavelength of 365 nm.

3. Results and discussion

3.1. Thickness measurement

Fig. 1 shows the variation of film thickness with respect to the various substrate temperatures. Thickness of the samples is varied between 220 and 860 nm. The film thickness is increased up to 860 nm for the substrate temperature (450 °C) then decreases. The decrease in film thickness at higher substrate temperature (500 °C) can be attributed to an increase in the rate of re-evaporation and diminishing transport of the species at higher temperature. Similar results were reported earlier by Krunks and Mellikov [25] and Caillaud et al. [26] for the ZnO thin films deposited by SPT.

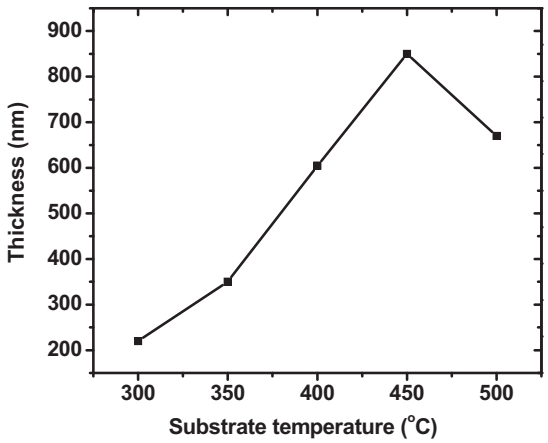

Fig. 1. Plot of thickness of ZnO thin films deposited at various substrate temperatures.

3.2. Structural properties

Fig. 2(a–e) shows the X-ray diffraction (XRD) patterns recorded over the 2θ values between 10° and 100° for the Zn_{300}, Zn_{350}, Zn_{400}, Zn_{450}, and Zn_{500} samples deposited onto the glass substrates from 0.4 M solution concentration. All films are polycrystalline and matches well with the hexagonal (wurtzite) crystal structure. All relatively sharp diffraction peaks can be well assigned to the hexagonal-phase, reported in the literature [27]. From XRD patterns, it is clear that deposited ZnO films have preferred orientation along (0 0 2) plane. Other orientations corresponding to (1 0 1), (1 0 2), (1 0 3), (1 1 2) and (0 0 4) planes are also present with low relative intensities as compared to that of (0 0 2) plane, indicating the preferred growth direction along *c*-axis.

As the substrate temperature increases, the peak intensity of (0 0 2) plane is increased progressively. This is due to increased film thickness and preferred growth. The slight decrement in (0 0 2) peak intensity at 500 °C is the combined effect of reduced film thickness and less deposition of the active mass onto the glass substrate. The film crystalline properties are characterized by the

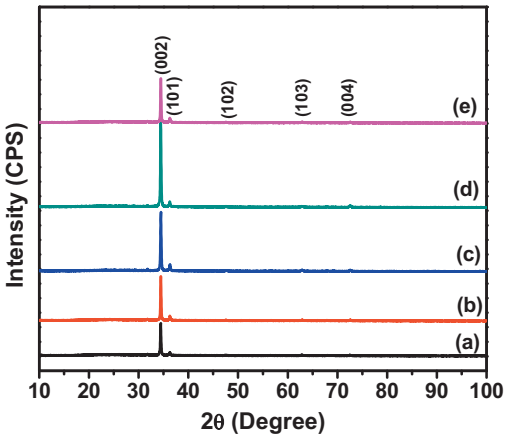

Fig. 2. XRD patterns of ZnO thin films obtained at various substrate temperatures (a) 300 °C (Zn_{300}), (b) 350 °C (Zn_{350}), (c) 400 °C (Zn_{400}), (d) 450 °C (Zn_{450}), and (e) 500 °C (Zn_{500}).

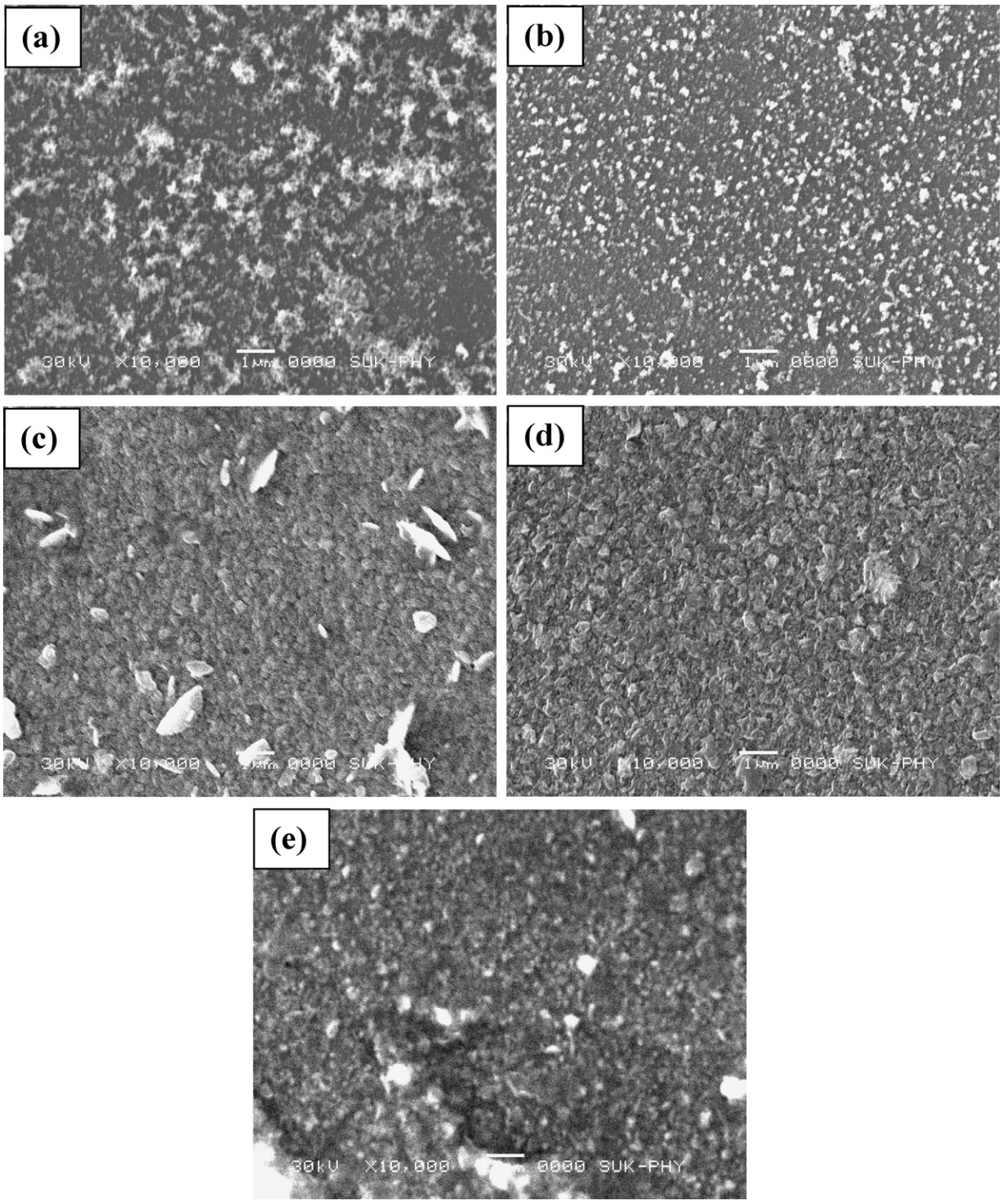

Fig. 3. SEM images of ZnO thin films obtained at substrate temperatures (a) 300 °C (Zn_{300}), (b) 350 °C (Zn_{350}), (c) 400 °C (Zn_{400}), (d) 450 °C (Zn_{450}), and (e) 500 °C (Zn_{500}).

crystallite size. The crystallite size was calculated by using the well-known Debye–Scherrer's formula. The calculated crystallite size varies between 28 nm and 41 nm for Zn_{300}–Zn_{500} samples. It is observed that, the crystallite size increases up to 41 nm for substrate temperature (450 °C) and then decreases for higher deposition temperature (500 °C). This indicates that the Zn_{450} sample has a good crystalline quality.

3.3. Morphological studies

Surface morphological study of the ZnO thin films was carried out using SEM. The recorded SEM images (10,000× magnification) of all the ZnO samples deposited at different substrate temperatures onto the glass substrates are shown in Fig. 3.

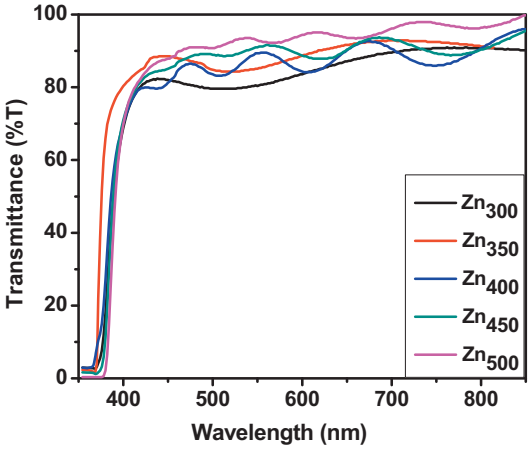

Fig. 4. Transmittance spectra of the ZnO thin films deposited at various substrate temperatures.

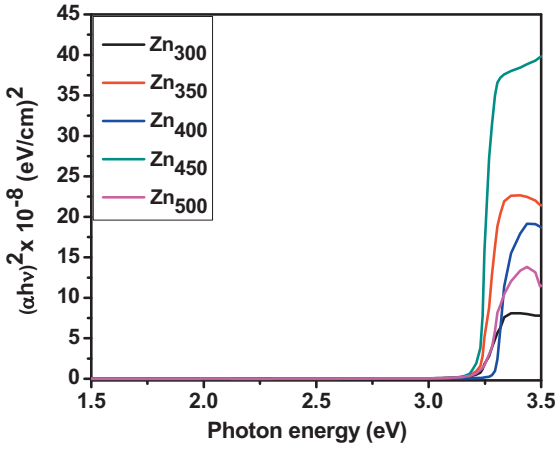

Fig. 5. Band gap energy of the ZnO thin films deposited at various substrate temperatures.

Several atomic rearrangement processes involved during the pyrolytic decomposition of the sprayed droplets onto the preheated substrates, which are responsible for the different surface topographies of the thin films. The nucleation process depends on the interfacial energies between the substrate surface and the condensing species and is governed by the substrate temperature. The surface mobility of the condensing species defines the crystallinity of the film. Generally, the species will diffuse through several atomic distances before sticking to a stable position. A high substrate temperature favors rapid and defect free growth of crystallites due to oxidation of Zn atoms and optimum surface diffusion of the species, whereas a low substrate temperature results in the growth of a disordered or a poorly crystallized structure. The development of a smooth, dense and uniform microstructure with good adhesion to the substrate was observed with the increase of substrate temperature.

The SEM micrographs show that, the surface morphology of the films is strongly dependent on the substrate temperature. An atomizer converts feedstock solution into the tiny aerosols. The aerosols are made up of zinc acetate and solvent. These aerosols encounter progressive increment in temperature which approaching towards heated substrates. As a result of which solvent evaporates, leaving behind solute containing zinc-acetate. Zinc acetate precipitate upon its pyrolytic decomposition causing zinc species to strike onto the substrates. Thermal oxidation of zinc leads to the formation of ZnO crystallites by following Stepple–Wronoki type growth model. This is a dynamic process and depends very much on the substrate temperature. At lower substrate temperature (300 °C), subsequent temperature gradient in the spray reactor is less. This causes the decomposition of zinc acetate inefficient and deposition of precipitate, rather than zinc species, takes place. Fig. 3(a) reveals the formation of non-uniform ZnO thin films onto the glass substrate. The degree of pyrolytic decomposition increases at 350 °C, causing relatively better droplet dynamics (Fig. 3(b)). Much improvement was observed at 400 °C (Fig. 3(c)) with no apparent formation of precipitate. An effective pyrolytic decomposition is accomplished forming zinc species just above the substrate. These zinc species get deposited onto the substrate for subsequent thermal oxidation to ZnO. However, some asperity is still visible and grain growth is uneven. The Zn_{450} sample shows the uniform and compact granular morphology with the tiny grains of the size ~60–80 nm size, as shown in Fig. 3(d). The diminished mass transport at higher substrate temperature (500 °C) shown in Fig. 3(e), causes deposition of less active mass and reduction in film thickness. This behavior is consistent with the results reported by Shinde et al. [28].

3.4. Optical properties

Fig. 4 shows the optical transmission spectra of ZnO thin films recorded over the wavelength range 350–850 nm. The films are highly transparent in the visible range of the electromagnetic spectrum with an average transmittance reaching values up to 85% and present a sharp ultraviolet cut-off at approximately 380 nm. The transmittance spectra are due to the light interference at the interface between the film and substrate materials [29].

The well-developed interference patterns in transmittance spectra show that the films are specular to a great extent. It is noticed that, the transmittance of the sample increases as the substrate temperature increases. An increase in the transmittance of ZnO films can be attributed to the removal of organic species on the film at higher temperature. The reduction of the transmittance of the T_{300} is attributed to strong scattering and absorption. The strong scattering resulted from the existence of grain boundaries, the point defect (i.e., V_O), and disorder in the ZnO films.

The optical band gap energy (E_g) is one of the important parameters that are very useful for the selection of the material to be used for a particular application and it can be estimated from optical absorption measurement. The optical absorption spectra of all the ZnO thin films were recorded over the wavelength range 350–850 nm at room temperature. The variation of $(\alpha h\nu)^2$ with photon energy ($h\nu$) is shown in Fig. 5. The optical absorption data were analyzed using the relation (1) of optical absorption in semiconductor near band edge.

$$\alpha = \frac{\alpha_0(h\upsilon - E_g)^n}{h\upsilon} \quad (1)$$

The value of band gap energies of the all samples lies in the range of 3.25–3.21 eV. Our results are in good agreement with the E_g values reported by Lokhande et al. [30] and Yoon and Cho [31].

3.5. Photoluminescence

A study of PL property of ZnO is very important because it can provide more valuable information on the quality and purity of the materials. Luminescence of ZnO phosphor has recently regained much interest because of its potential use in new low-voltage fluorescence applications, such as field emission display technologies [32]. Fig. 6 shows the room temperature PL spectra of the ZnO thin films. In PL spectra, a strong UV emission at around 398 nm with two shoulder peaks at 382 nm and 410 nm are observed. Moreover, a weak blue emission at 471 nm and green emission at 520 nm are observed. The luminescent band at 398 nm

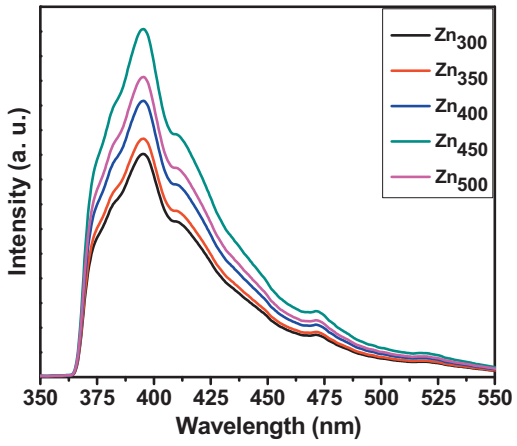

Fig. 6. Photoluminescence spectra of all the samples deposited at various substrate temperatures.

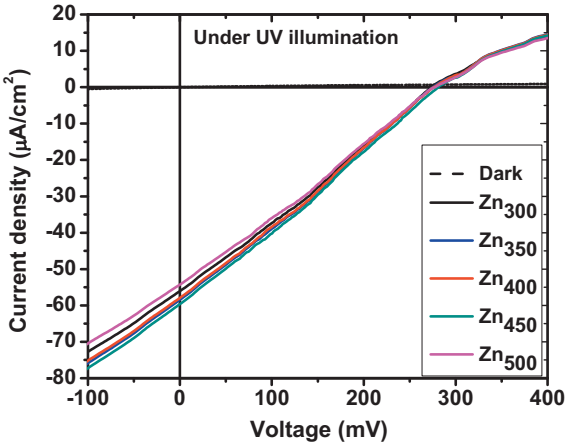

Fig. 7. *I–V* curves of the all samples deposited at various substrate temperatures under UV illumination.

corresponds to the band edge transition of ZnO material. The presence of this band is an indicator of the good crystallinity. The peak centered at 520 nm with weak intensity, is the characteristic of blue-green emission which is also typical for ZnO material. According to Vanheusden et al. [32] and Egelhaaf and Oelkrug [33], this peak corresponds to a defect-related luminescence (deep-level luminescence), due to the oxygen vacancies in ZnO. This defect-related luminescence is explained by radiative transitions between shallow donors (oxygen vacancies) and deep acceptors (Zn vacancies). The blue emission was also reported previously by Wu and Liu [34]. In this case, the acceptor level is located 2.5 eV below the conduction band edge [35], while the donor level is known as a shallow level at 0.05–0.19 eV, leading to an emission band centered around 508–540 nm. Furthermore, Minami et al. [36] proposed that the blue–green emission in this material might be associated to a transition within a self-activated centre formed by a double-ionized zinc vacancy $(V_{Zn})^{-2}$ and a single-ionized interstitial Zn^{+} at the one and/or two nearest-neighbor interstitial sites. A low level of oxygen defect density is observed from PL spectrum with sharp UV emission. The intensity of the UV emission of ZnO films is dependent on the microcrystalline structure and stoichiometry [32]. Proper substrate temperature is favorable for the migration of atoms to favorable positions and the enhancement of crystallinity. It will decrease the concentration of intrinsic defects and improve the NBE luminescence efficiency. Hence, the peak intensity of the UV emission is increases as the substrate temperature increases up to 450 °C and then decreases for higher temperature at 500 °C.

However, at excessively high growth temperature (500 °C), zinc acetate decomposes before reaching the surface of substrate, which may induce smaller crystal size and more grain interface as the size limit of individual droplet in air. Above the deposition temperature of 450 °C, the Zn evaporation in ZnO films may occur and consequently degrade the stoichiometry of ZnO films [37]. Therefore, the PL intensity for the Zn_{500} sample decreases, which is related to the thermally activated nonradiative recombination mechanism. We believe that, the nonradiative recombination centres are generated by the oxygen vacancies which increase with increasing substrate temperature. From PL spectra, it is concluded that the Zn_{450} sample has good crystalline quality and have less defect density. Such spray deposited ZnO thin films are one of the promising candidates for the UV optical devices.

3.6. Photoelectrochemical properties

Recently, PEC solar cells with active semiconductor–electrolyte junction are considered to be efficient solar energy harvester and intensive research is going on to use such systems in photosplitting of water for the production of hydrogen – a much cleaner substitute of fossil fuels. The viability of solar power as an alternative source of energy relies on establishing low-cost, large-area manufacturing processes. These would most likely be achieved by adopting cells based on a thin film technology. Thin film-based PEC solar cells have wide applications due to their low fabrication cost, high-throughput processing techniques and ease of junction formation with an electrolyte [18–23,28]. Therefore, PEC solar cells with semiconductor under investigation can be used as a simple and quick technique to test the quality of solar cell materials.

PEC is a new, reliable and unique technique in thin film technology, which has proven to be a best tool for optimization of preparative and post preparative parameters of the semiconducting electrodes prepared by any deposition technique [38]. The PEC performance of the all ZnO thin films deposited at various substrate temperatures was checked with the help of three electrode configuration. In dark and under UV illumination, the current–voltage (*I–V*) characteristics of 'glass/ITO/ZnO/SCE' cells were measured.

After illumination of the light, the junction is formed using above configuration in a PEC cell, the magnitude of the open circuit voltage increases with the negative polarity towards the ZnO thin film, indicating cathodic behavior of photovoltage which confirms that spray deposited ZnO films are of *n*-type [39].

The output parameters of the PEC solar cell i.e. the efficiency, η (%) and FF are calculated from the following relations (2) and (3).

$$\eta(\%) = \frac{I_m V_m}{P_{in}} \times 100 \quad (2)$$

$$FF = \frac{I_m V_m}{I_{SC} V_{OC}} \quad (3)$$

where P_{in} is the input light intensity, I_{sc} is the short circuit current and V_{oc} is the open circuit voltage. I_m and V_m are the values of maximum current and maximum voltage, respectively that can be extracted from an output characteristic of the PEC solar cell.

I–V characteristics of the all samples, when illuminated under UV light are shown in Fig. 7. From the *I–V* measurements, it is observed that the values of I_{sc} (60 μA cm^{-2}), V_{oc} (280 mV) are obtained for the ZnO thin films under UV illumination using 0.5 M Na_2SO_4 as an electrolyte. The compact and densely packed ZnO crystallites can absorb enough light. Furthermore, the photogenerated electrons can transport directly through crystallites and compact layers to the conducting substrates with minimum loss. This greatly reduces the recombination losses of photogenerated charge carriers due to decrement in grain boundary resistance in the charge transportation process. The obtained output parameters

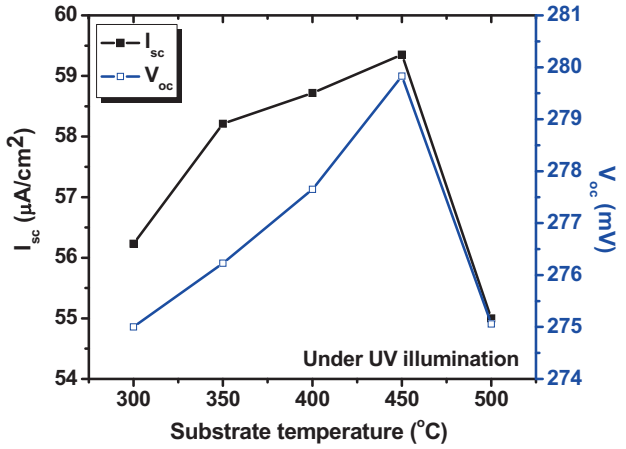

Fig. 8. Plot of the variation of output parameters (I_{sc} and V_{oc}) of all samples illuminated under UV light with various substrate temperature.

of the PEC solar cell by using different ZnO photoanodes illuminated under UV light are shown in Fig. 8.

It is observed that, the sample Zn_{450} shows better performance related to other ZnO films. This is because of the more thickness (860 nm) and lower value of band gap energy, which absorbs the enough light as compared to other samples. The optimized parameters for the deposition of the PEC active ZnO thin films were depicted in Table 1.

4. Conclusions

ZnO thin films were synthesized by using a simple, cost effective SPT onto the glass and ITO coated glass substrates at various substrate temperatures in the range of 300–500 °C. The films were polycrystalline with (0 0 2) preferential orientation in all the cases. The calculated crystallite size was found in the range of 28–41 nm. The surface morphology of the films is strongly dependent on substrate temperatures. From SEM micrographs, it is observed that the entire surface of the substrate is covered with tiny spherical grains of 80–90 nm grain size. The films were highly transparent with average transmittance 85% having band gap energy 3.25 eV. All samples exhibit room temperature PL. A strong UV emission at 398 nm with weak green emission at 520 nm is observed in the PL spectra. From PL spectra, it is concluded that the sample Zn_{450} has good crystalline quality and have less defects. Such spray deposited ZnO thin films are one of the promising candidates for the UV optical devices. Among the studied samples, the film prepared at the substrate temperature, 450 °C (sample Zn_{450}) shows highest output parameters like I_{sc}, V_{oc} and FF under UV illumination.

Acknowledgements

Authors wish to acknowledge the University Grants Commission (UGC), New Delhi, India for the financial support through the UGC-DRS-II phase, ASIST programmes and Department of Science and Technology through DST-FIST programme. One of the authors NLT wish to acknowledge the UGC for Research Fellowship in Sciences for Meritorious Students.

References

[1] X.Y. Kong, Z.L. Wang, Nano Lett. 3 (2003) 1625.
[2] Y.-S. Fu, J. Sun, Y. Xie, J. Liu, H.-L. Wang, X.-W. Du, Mater. Sci. Eng. B 166 (2010) 196.
[3] J.B. Baxter, E.S. Aydil, Appl. Phys. Lett. 86 (2005) 053114.
[4] A. Umar, Nanoscale Res. Lett. 4 (2009) 1004.
[5] K.V. Gurav, V.J. Fulari, U.M. Patil, C.D. Lokhande, O.S. Joo, Appl. Surf. Sci. 256 (2010) 2580.
[6] Z. Fan, J.G. Lu, J. Nanosci. Nanotechnol. 5 (2005) 1561.
[7] N.L. Tarwal, P.S. Patil, Electrochim. Acta 56 (2011) 6510.
[8] T. Prasada Rao, M.C. Santhosh Kumar, A. Safarulla, V. Ganesan, S.R. Barman, C. Sanjeeviraja, Phys. B: Condens. Matter 405 (2010) 2226.
[9] I. Stambolova, V. Blaskov, M. Shipochka, S. Vassilev, C. Dushkin, Y. Dimitriev, Mater. Chem. Phys. 121 (2010) 447.
[10] A.E. Hichou, M. Addouc, J. Ebothe, M. Troyon, J. Lumin. 113 (2005) 183.
[11] R. Ayouchi, F. Martin, D. Leinen, J.R. Ramos-Barrado, J. Cryst. Growth 247 (2003) 497.
[12] T. Dedova, J. Klauson, C. Badre, Th. Pauporté, R. Nisumaa, A. Mere, O. Volobujeva, M. Krunks, Phys. Stat. Sol. A 205 (2008) 2355.
[13] U. Alver, T. Kılınc, E. Bacaksız, S. Nezir, Mater. Chem. Phys. 106 (2007) 227.
[14] M. Krunks, T. Dedova, I. Oja Açik, Thin Solid Films 515 (2006) 1157.
[15] A.T. Mosbah, A. Moustaghfir, S. Abed, N. Bouhssira, M.S. Aida, E. Tomasella, M. Jacquet, Surf. Coat. Tech. 200 (2005) 293.
[16] K. Liu, B.F. Yang, H. Yan, Z. Fu, M. Wen, Y. Chen, J. Zuo, Appl. Surf. Sci. 255 (2008) 2052.
[17] A. Bouzidi, N. Benramdane, H. Tabet-Derraz, C. Mathieu, B. Khelifa, R. Desfeux, Mater. Sci. Eng. B 97 (2003) 5.
[18] V.M. Aroutiounian, V.M. Arakelyan, G.E. Shahnazaryan, Sol. Energy 78 (2005) 581.
[19] J. Yuan, M. Chen, J. Shi, W. Shangguan, Int. J. Hydrogen Energy 31 (2006) 1326.
[20] D.-M. Tang, G. Liu, F. Li, J. Tan, C. Liu, G.Q. Lu, H.-M. Cheng, J. Phys. Chem. C 113 (2009) 11035.
[21] K.-S. Ahn, Y. Yan, S. Shet, T. Deutsch, J. Turner, M. Al-Jassim, Appl. Phys. Lett. 91 (2007) 231909.
[22] K.-S. Ahn, S. Shet, T. Deutsch, C.-S. Jiang, Y. Yan, M. Al-Jassim, J. Turner, J. Power Sources 176 (2008) 387.
[23] M. Gupta, V. Sharma, J. Shrivastava, A. Solanki, A.P. Singh, V.R. Satsangi, S. Dass, R. Shrivastav, Bull. Mater. Sci. 32 (2009) 23.
[24] N.L. Tarwal, P.S. Patil, Appl. Surf. Sci. 256 (2010) 7451.
[25] M. Krunks, E. Mellikov, Thin Solid Films 270 (1995) 33.
[26] F. Caillaud, A. Smithand, J.-F. Baumard, J. Eur. Ceram. Soc. 6 (1990) 313.
[27] H. Gomez, M. de la, L. Olvera, Mater. Sci. Eng. B 134 (2006) 20.
[28] S.S. Shinde, P.S. Patil, R.S. Mane, B.N. Pawar, K.Y. Rajpure, J. Alloys Compd. 503 (2010) 416.
[29] Y.M. Lu, C.M. Chang, S.I. Tsai, T.S. Wey, Thin Solid Films 56 (2004) 447.
[30] B.J. Lokhande, P.S. Patil, M.D. Uplane, Mater. Lett. 57 (2002) 573.
[31] K.H. Yoon, J.Y. Cho, Mater. Res. Bull. 35 (2000) 39.
[32] K. Vanheusden, C.H. Seager, W.L. Warren, D.R. Tallant, J.A. Voigt, Appl. Phys. Lett. 68 (1996) 403.
[33] H.J. Egelhaaf, D. Oelkrug, J. Crystal Growth 161 (1996) 190.
[34] J.J. Wu, S.C. Liu, Adv. Mater. 14 (2002) 215.
[35] E.G. Bylander, J. Appl. Phys. 49 (1978) 1188.
[36] T. Minami, H. Nanto, S. Takata, J. Lumin. 24/25 (1981) 63.
[37] P.M. Ratheesh Kumar, C. Sudha Kartha, K.P. Vijayakumar, J. Appl. Phys. 98 (2005) 023509.
[38] R.R. Sawant, K.Y. Rajpure, C.H. Bhosale, Phys. B: Condens. Matter 393 (2007) 249.
[39] P.S. Shinde, P.S. Patil, P.N. Bhosale, C.H. Bhosale, J. Am. Ceram. Soc. 91 (4) (2008) 1266.